IOPscience iopscience.iop.org

Home Search Collections Journals About Contact us My IOPscience

Mechanism of Aluminum Induced Lateral Crystallization of Amorphous Silicon

This content has been downloaded from IOPscience. Please scroll down to see the full text.

2010 Jpn. J. Appl. Phys. 49 095601

(http://iopscience.iop.org/1347-4065/49/9R/095601)

View the table of contents for this issue, or go to the journal homepage for more

Download details:

IP Address: 140.113.38.11

This content was downloaded on 25/04/2014 at 06:07

Please note that terms and conditions apply.

Mechanism of Aluminum Induced Lateral Crystallization of Amorphous Silicon

Shih-Yang Huang, Chuan-Chi Wang[1], Chih-Lung Lin, Yu-Lin Tsai, Cheun-Guang Chao[1], and Tzeng-Feng Liu*

Department of Materials Science and Engineering, National Chiao Tung University, Hsinchu City 300, Taiwan, R.O.C.
[1]*Department of Management Information System, Chin Min Institute of Technology, Miaoli County 351 Taiwan, R.O.C.*

Received February 12, 2010; accepted June 26, 2010; published online September 21, 2010

The aluminium-induced lateral crystallization (AILC) of amorphous silicon (a-Si) on a glass substrate has been investigated. By means of a photoresist-based process, Al islands (100 nm) were thermally evaporated using 15 V, 3.5 A, and 25 V, 5.6 A on the a-Si layer (100 nm), which was deposited on a glass substrate. SEM examinations indicated that the Al islands exhibited smooth and crystalline-grain morphology. Annealing processes were carried out at 748 and 823 K for various times. After annealing, AILC could be clearly observed in the crystalline-grain sample, but not in the smooth sample. TEM analyses showed that the mechanism of AILC resulted from two layer exchange processes. First, the Al islands exchanged with the underlying a-Si layer vertically during AIC, and then the generation of Al particles accompanying AIC caused a lateral layer exchange with the remaining a-Si layer with further annealing. © 2010 The Japan Society of Applied Physics

DOI: 10.1143/JJAP.49.095601

1. Introduction

Polycrystalline silicon (poly-Si) has attracted much attention for application in electronic devices such as thin-film transistors[1)] and thin-film solar cells owing to its high device reliability and good electrical performance.[2)] Both laser crystallization and solid-phase crystallization (SPC) are the most widely used methods for poly-Si preparation.[3,4)] However, laser crystallization remains an expensive and complex process, while SPC suffers from long annealing time even at typically 873 K, which is still too high for large-area glass substrates.

Metal-induced crystallization (MIC) has been reported to successfully lower the crystallization temperature down to 773 K, where eutectic forming metals, such as Au and Al, or silicide forming metals, such as Pd and Ni, have been added to amorphous silicon (a-Si) to enhance the nucleation rate.[5–7)] In order to further lower metal contamination and obtain large-grained poly-Si films, metal-induced lateral crystallization (MILC) has been developed.[8,9)] Most MILC has been studied using metals that form silicides with Si such as Ni. In addition to the extensive studies of aluminum-induced crystallization (AIC),[10–14)] a few studies have focused on MILC using metals that remains to be clarified form eutectics such as Al.[15,16)] However, the mechanism of AILC is not clear yet. Therefore, the purpose of this work is to elucidate the mechanism of AILC.

2. Experimental Procedure

A-silicon films with a thickness of 100 nm were deposited by plasma-enhanced chemical vapor deposition on a glass substrate. The samples were treated by a photolithographic process, and then a thin Al layer with a thickness of 100 nm was thermally evaporated on the a-Si surface under the conditions of 15 V, 3.5 A (sample 1) and 25 V, 5.6 A (sample 2). The deposition rates of Al for sample 1 and 2 were 0.677 and 20 nm/s, respectively. After evaporation, the Al layer on the top of the photoresist patterns was removed by the lift-off method and only the Al layer (Al islands) evaporated directly on the a-Si was left. The cross-sectional structure of the sample after removing the photoresist patterns is illustrated in Fig. 1. The conventional annealing processes were performed at 748 and 823 K for various times

*E-mail address: tfliu@cc.nctu.edu.tw

Fig. 1. Illustration of the cross-sectional structure of the sample after removing the photoresist patterns.

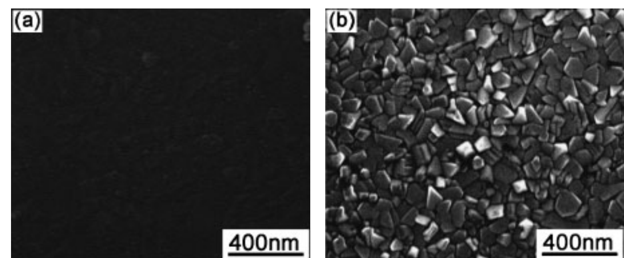

Fig. 2. SEM images showing the surface morphology of the Al layer deposited under the following conditions: (a) 15 V, 3.5 A (sample 1) and (b) 25 V, 5.6 A (sample 2).

in a vacuum heat-treated furnace. To investigate the bare poly-Si formed during annealing, the remaining Al on the surface was etched off using a standard Al etching solution (80% phosphoric acid, 5% nitric acid, 5% acetic acid, and 10% deionized water). Optical microscopy (OM), scanning electron microscopy (SEM: JEOL-JSM6500FX), and transmission electron microscopy (TEM: JEOL-2100F) were carried out for microstructural characterization. The cross-sectional TEM specimens were prepared using an FEI FIB200xP focused ion beam microscope.

3. Results and Discussion

Figures 2(a) and 2(b) respectively show the surface morphology of samples 1 and 2 before the annealing treatment, revealing that the surface morphology of sample 2 is much rougher than that of sample 1. Moreover, clear crystalline grain boundaries of Al can clearly be seen in sample 2, but not in sample 1. After annealing at 748 K for 5 h, the crystallization results of samples 1 and 2 are shown in Figs. 3(a) and 3(b), respectively. In Fig. 3, it is evident that AIC induced in the area where a-Si was in contact with Al islands (marked as "A") can be observed in both samples. However, AILC induced in the channel region where the Al

 © 2010 The Japan Society of Applied Physics

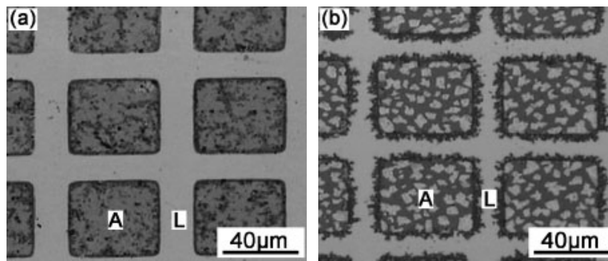

Fig. 3. OM images of (a) sample 1 and (b) sample 2 annealed at 748 K for 5 h.

layer was not deposited (marked as "L") is only seen in sample 2 and no evidence of AILC can be detected in sample 1. To evaluate the effect of temperature on lateral crystallization, sample 2 was annealed at 748 and 823 K for various times. The relationship between the laterally crystallized area ratio (lateral crystallization area, total area of channel) and the annealing time is shown in Fig. 4(a). The laterally crystallized area ratio reached 1 in 5 min at 823 K but only 0.7 at 748 K for 9 h. Figures 4(b) and 4(c) show two typical scanning electron micrographs of sample 2 annealed at 748 and 823 K for 1 h, respectively. A-Si was transformed into poly-Si by AILC under both conditions. The crystallization rates of AILC are about 2 μm/min at 823 K and 0.013 μm/min at 748 K. Evidently, annealing temperature is an important factor that affects the growth rate of lateral crystallization.

The layer exchange mechanism of the AIC process was well established in many studies.[10–14] In addition, AILC has been reported by Rui *et al.*[15] and Abbassi *et al.*[16] They found AILC and established the model of AILC. However, the mechanism of AILC remains unclear. Therefore, cross-sectional TEM analyses of the area marked as "T" in Fig. 4(c) were performed to examine the crystal structure of the laterally crystallized poly-Si layer in this study. Figure 5(a) shows a bright-field (BF) electron micrograph of the cross-sectional structure of sample 2 annealed at 823 K for 1 h. The white area on the top of this figure (marked F) was removed by FIB during the cross-sectional sample preparation. Figures 5(b) and 5(c) are two selected-area diffraction patterns (SADPs) taken from the "L" area in Fig. 5(a), indicating that the crystal structure has a diamond structure with a lattice parameter $a = 0.542$ nm, which corresponds to that of poly-Si. Accordingly, the microstructure of the grains present in the AIC and AILC areas should be poly-Si. In Fig. 5(a), some coarse particles can also be observed at the interface between Al islands and poly-Si grains as well as at the grain boundary of poly-Si grains. Shown in Fig. 5(d) is a SADP taken from a coarse particle marked "p" in Fig. 5(a). From the camera length and the measurements of angles and d-spacings of the

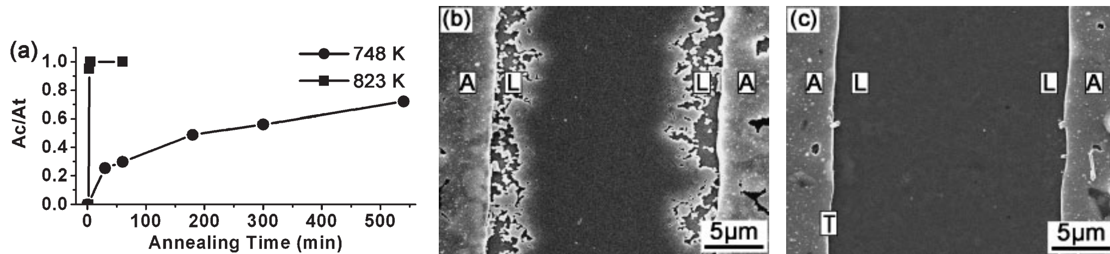

Fig. 4. (a) Relationship between the laterally crystallized fraction (Ac/At, Ac: laterally crystallized area, At: total area of the channel) and annealing time for sample 2 annealed at 748 and 823 K for various times. SEM images of sample 2 annealed at (b) 748 K and (c) 823 K for 1 h.

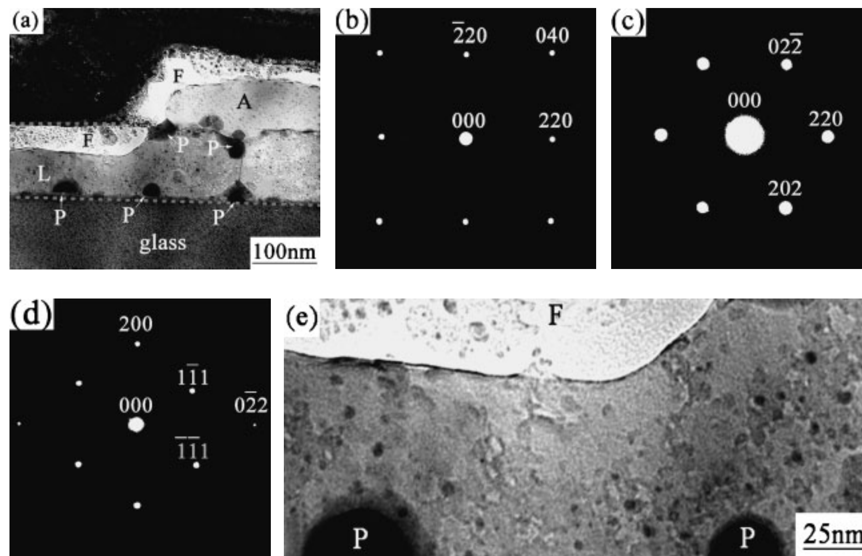

Fig. 5. Cross-sectional TEM images of the lateral crystallized poly-Si layer of sample 2 annealed at 823 K for 1 h: (a) BF. (b) and (c) two SADPs taken from the "L" area in (a). The zone axes of the poly-Si are (b) [001] and (c) [$\bar{1}$11]. (d) SADP taken from a particle marked "P" in (a). The zone axis of Al is [011]. (e) BF, high magnification image of (a).

 © 2010 The Japan Society of Applied Physics

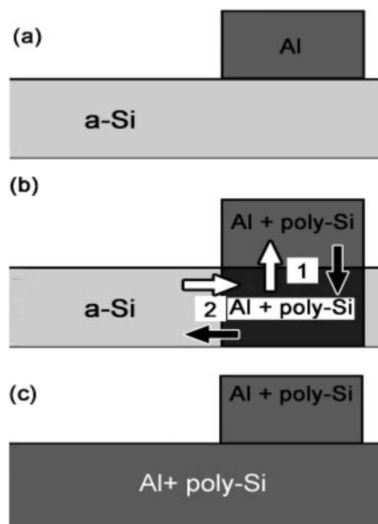

Fig. 6. Schematic illustration of the AILC mechanism (➡: diffusion of Al atoms; ⇨: diffusion of Si atoms).

diffraction spots, the crystal structure of the particle was found to be consistent with that of Al. Figure 5(e), a higher magnification of Fig. 5(a), reveals that many small particles with diameters of 2–5 nm were formed within poly-Si grains. Electron diffraction analysis demonstrated that the small particles were also Al. It is therefore considered that when the sample was annealed, the Al diffused into the adjacent a-Si layer during the layer exchange and Al particles were formed owing to the very low solid solubility of Al in Si.

On the basis of the above observations, it is reasonable to suggest that the mechanism of AILC results from two layer exchange processes. First, the Al islands are replaced vertically with the underlying a-Si layer during AIC, and then the generated Al particles accompanying AIC poly-Si cause a lateral layer exchange with the a-Si layer of the "L" area with further annealing. The schematic illustration of the AILC is shown in Fig. 6. In addition, TEM examinations revealed that the number of tiny Al particles was much greater in sample 2 than that in the sample 1. This implies that the rate of interdiffusion between Al islands and the a-Si layer (AIC) in sample 2 is much higher than that in sample 1. The reason for this may be that the surface of sample 2 had obvious crystalline grain boundaries for Si atoms to easily diffuse along grain boundaries in Al. The grain boundaries of the Al islands were necessary agents for the initiation of the crystallization of Si, and then Al was repelled from the Si grains and diffused into adjacent a-Si layer. The number of small Al particles in the Si layer under Al islands in sample 1 was insufficient. Therefore, the lateral layer exchange would have been very slow. Consequently, the AILC of sample 1 under all the annealing conditions could not be observed in the present study.

4. Conclusions

AILC can be observed only in sample 2 with a grainy Al layer on an a-Si layer, but not in sample 1 with a smooth Al layer on an a-Si layer. This indicates that the surface morphology of evaporated Al has a marked effect on the lateral crystallization of poly-Si. The mechanism of AILC results from two layer exchange processes. The vertical layer exchange and the horizontal layer exchange. The crystallization rate of AILC reaches 2 μm/min at 823 K but only 0.013 μm/min at 748 K. Evidently, the annealing temperature is another important factor that affects the velocity of lateral crystallization.

Acknowledgement

The authors are pleased to acknowledge the financial support of Wintek Corporation to this research.

1) J. P. Lu, K. V. Schuylenbergh, J. Ho, Y. Wang, J. B. Bruce, and R. A. Street: Appl. Phys. Lett. **80** (2002) 4656.
2) K. R. Catchpole, M. J. McCann, K. J. Weber, and A. W. Blakers: Sol. Energy Mater. Sol. Cells **68** (2001) 173.
3) R. B. Bergmann, G. Oswald, M. Albrecht, and V. Gross: Sol. Energy Mater. Sol. Cells **46** (1997) 147.
4) F. A. Quli and J. Singh: Mater. Sci. Eng. B **67** (1999) 139.
5) E. A. Guliants, W. A. Anderson, L. P. Guo, and V. V. Guliants: Thin Solid Films **385** (2001) 74.
6) S. W. Lee, Y. C. Jeon, and S. K. Joo: Appl. Phys. Lett. **66** (1995) 1671.
7) H. H. Abu-Safe, A.-K. M. Sajjadul-Islam, H. A. Naseem, and W. D. Brown: Mater. Res. Soc. Symp. Proc. **910** (2006) A21.09.
8) S. W. Lee and S. K. Joo: IEEE Electron Device Lett. **17** (1996) 160.
9) Z. Jin, G. A. Bhat, M. Yeung, H. S. Kwok, and M. Wong: J. Appl. Phys. **84** (1998) 194.
10) O. Nast: J. Appl. Phys. **88** (2000) 716.
11) J. Y. Wang, D. He, Y. H. Zhao, and J. Mittemeijer: Appl. Phys. Lett. **88** (2006) 061910.
12) J. Schneider, J. Klein, M. Muske, S. Gall, and W. Fuhs: Appl. Phys. Lett. **87** (2005) 031905.
13) O. Nast and S. R. Wenham: J. Appl. Phys. **88** (2000) 124.
14) G. Ekanayake and H. S. Reehal: Vacuum **81** (2006) 272.
15) Y. Liu, M. D. Deal, M. Sultana, and J. D. Plummer: Mater. Res. Soc. Symp. Proc. **762** (2003) A16.2.1.
16) M. S. Abbasi, H. Abu-Safe, H. Naseem, and D. Brown: Mater. Res. Soc. Symp. Proc. **808** (2004) A4.26.1.

© 2010 The Japan Society of Applied Physics